

**DEGRADATION OF AZO DYE C. I. DIRECT VIOLET- 4 BY VANADIUM  
MODIFIED MFI ZEOLITE POWDER ADSORPTION AND  
PHOTOOXIDATION IN AQUEOUS SOLUTION**

---

MOHAMED S. THABET

*.Department of Chemistry, Faculty of Science, Al-Azhar University, Cairo, Egypt*

E-mail address: [thabet1972@yahoo.com](mailto:thabet1972@yahoo.com)

---

**Abstract**

Vanadium modified zeolite was synthesized using the chemical liquid deposition (CLD) and wet exchange methods refer by  $V/Z_{CLD}$ ,  $V/Z_{wet}$ . The obtained materials were calcined at 550°C and characterized using XRD, FTIR, and nitrogen adsorption. The characterized materials were applied for the photo-decolorization of direct violet-4 (DVO-4) as a member of azo dye family, in aqueous medium using hydrogen peroxide and/or UV irradiation (254 nm). The effects of time and catalyst concentration on the decolorization of DVO-4 dye were investigated. The decolorization of (DVO-4) dye and the decreasing in concentration of the dye have been followed using UV-vis spectrophotometry. Results showed that the addition of  $V/Z_{CLD}$ ,  $V/Z_{wet}$  and  $H_2O_2$  to the dye solution enhanced the rate of degradation. The decolorization followed the pseudo first order kinetics model and a significant mineralization of (DVO-4) was observed.

**Keywords:** Photocatalysis; Direct Violet; Azo dye; Decolorization; Vanadium; MFI zeolite

**Introduction**

Azo dyes are a versatile class of colored organic compounds that have extensively been used in both industry for applications such as textiles, papers, leathers, gasoline, additives, foodstuffs and cosmetics and analytical chemistry [1,2]. These azo dyes are known to be largely non-biodegradable in aerobic conditions and to be reduced to more hazardous intermediates in anaerobic conditions [3].

It is well known that soluble azo dyes when incorporated into the body are split into corresponding aromatic amines by liver enzymes and intestinal flora, which can cause cancer in human [4], from wastes is often more important than the other colorless organic substances because the presence of small amounts of dyes (below 1 ppm) is clearly visible and influences the water environment considerably. Therefore, it is necessary to find an effective method of wastewater treatment in

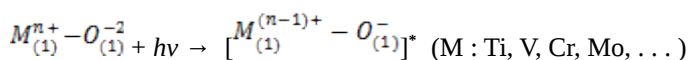
order to remove color from textile effluents [5]. One of the new methods of wastewater treatment containing dyes is their photocatalytic degradation in solutions illuminated with UV irradiation, which contains a suitable photocatalyst.

Heterogeneous photocatalytic oxidation (PCO) for wastewater treatment has received much attention by various research groups. Numerous types of catalysts and contaminants have been investigated on laboratory scale [6,7]. However, very few commercial applications of this technology are available at present. One of the major reasons is the deactivation of the photocatalyst when photocatalysis is utilized to treat real wastewater [8].

Many successful cases for activation of  $H_2O_2$  by transition metal in zeolites are well demonstrated in the heterogeneous catalysis. ZSM-5 zeolite, with highly ordered micropores, surface acidity, and ion-exchange capacities, is one of the most widely applied inorganic materials as catalyst support, adsorbent, and molecular-sized space for various chemical or photochemical reactions [9–11].

The transition metal ions in metallosilicate catalysts are considered to be highly dispersed at the atomic level and well defined, existing in a specific structure of the zeolite framework. According to the Löwenstein rules, the Al atoms within the zeolite framework cannot connect with each other directly, a property observed in most zeolites. If this is also the case for metallosilicate zeolites, the well-prepared zeolite sample should contain only isolated metal ions in their framework structures. This phenomenon is of great significance in the design of highly dispersed transition metal oxides such as Ti, V, Cr, Mo, etc. which can be excited under UV-irradiation to form the corresponding charge-transfer excited state involving an electron transfer

from  $O_{(1)}^-$  to  $M_{(1)}^{n+}$  :



The high reactivities of these charge-transfer excited states, i.e. electron-hole pair states, which are localized quite near to each other as compared to the electron and hole produced in semiconducting materials, induce various significant photocatalytic reactions. Zeolites having transition metal cations in their frameworks have been the

focus of much attention for their interesting and distinctive properties. So far, several types of such vanadium silicalite have been developed [12–15], and, the true chemical nature and reactivities of the vanadium silicalites, especially their photochemical properties.

In this work, ZSM-5 zeolite was selected as a support for dispersing the transition metal  $V_2O_5$  with 10% and 20% loading content as a non-conventional photocatalyst. Photoactivity of the catalysts is evaluated using the photocatalytic oxidation of DVO-4 dye. The physicochemical properties of vanadium containing ZSM-5 catalysts prepared by wet exchange and CLD methods were evaluated by surface area, XRD, and FTIR to identify the local structure of zeolite and correlating it with their photocatalytic activities.

## **Experimental**

### **Catalyst preparation**

#### **Preparation V-ZSM-5 by CLD (chemical liquid deposition) method.**

The impregnated V–ZSM-5 samples were prepared by mixing a calculated amount of ZSM-5 (CBr 8014, Lot no. 8014-08-D; Si/Al = 80) with an aqueous solution of ammonium metavanadate ( $NH_4VO_3$ , ADWIC) to give 10 and 20 wt. % of V/ZSM-5. The solution was refluxed at 80 °C for 3 h. and kept in air at 80 °C to complete the evaporation of water. The obtained products were dried at 110 °C for 2 h. The obtained solid was then calcined at 550 °C in air for 6 h.

#### **Preparation of V- ZSM-5 zeolite by wet exchange method.**

The V-ZSM-5 catalysts were prepared by the conventional aqueous cation wet exchange method.  $NH_4$ -ZSM-5 (CBr 8014) was wet exchanged with 500 ml of  $NH_4VO_3$  aqueous solution of known concentrations for 24 h at 80°C. [16] The resulting samples 10 and 20 wt.% of V/ $Z_{wet}$  loading percentage were filtered off, washed with distilled water, dried at 120 °C for 6 h and lastly calcined at 550°C for 6 h.

### **Catalyst characterization**

#### **X-ray Diffraction**

The X-ray diffraction (XRD) patterns of various prepared samples were performed using a Philips diffractometer (PW 3710) with Ni-filtered copper radiation ( $k = 1.5404\text{\AA}$ ) at 30 kV and scanning speed rate of  $2\theta = 2.5^\circ/\text{min}$ . The crystal size of the prepared materials was determined using the Scherrer equation [17]. The crystallinity of the prepared samples were calculated using the ratio of the sum of the areas of the most intense peaks for ZSM-5 samples ( $2\theta = 23^\circ$ ,  $23.8^\circ$  and  $24.3^\circ$ ) to that the same peaks for the standard (ZSM-5 Mobil Chemicals) and multiplying by 100.

### IR measurement

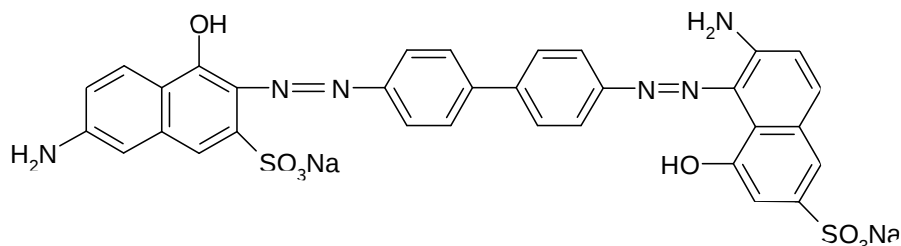
IR spectra were recorded in the solid state as KBr pellet on Bruker (Vector 22), single beam spectrometer at room temperature.

### Nitrogen adsorption

The nitrogen adsorption isotherms were measured at  $-196^\circ\text{C}$  using a conventional volumetric apparatus. The specific surface area was obtained using the BET method. The surface texture characteristic was obtained from both the BET isotherm and the  $V_{t-t}$  plots.

### Catalytic activity tests

The evaluation of the photoactivity was carried out in a cylindrical Pyrex glass reactor. A magnetic stirrer was used continuously to guarantee the good mixing of the solution. Irradiation experiments were performed using a 6W medium pressure Hg lamp (254 nm). Unless otherwise stated, the reaction was carried out at room temperature under the conditions of 0.3 g/l of the solid catalyst in 100 ml solution of 50 ppm DVO-4 dye, 61.6 mmol/l of  $\text{H}_2\text{O}_2$ . The degradation of DVO-4 dye was analyzed by UV-Vis spectrophotometer (JASCO V-570 unit, serial no. 29635) in the range of 190–800 nm. The degradation was determined at the wavelength of maximum absorption (525 nm).



**Structure of direct violet -4 dye (Chemical formula:  $C_{32}H_{22}N_6S_2O_8Na_2$ ; M.wt. = 432)**

In agreement with previous literatures [18, 19], the degradation of DVO-4 dye fitted with pseudo-first order kinetics [ $\ln(C/C_0) = -kt$ ] (where  $C_0$  and  $C$  are the initial dye concentration and at time  $t$ , respectively, and  $(k, \text{min}^{-1})$ , is the reaction rate constant). The rate constant,  $k$ , was calculated from the slopes of the straight-line portion of the plots [ $\ln(C/C_0)$  vs. time].

**Results and discussion**

**XRD**

XRD patterns of  $V/Z_{\text{CLD}}$  and  $V/Z_{\text{wet}}$  samples in comparison with that of parent ZSM-5 are depicted in Fig.1. The pattern of  $V/Z_{\text{wet}}$  sample seems to be similar to that of ZSM-5 emphasizing a high dispersion of vanadium ions in compensating positions inside the zeolite.  $V/Z_{\text{wet}}$  samples indicates the absence of any diffraction line characteristics for  $V_2O_5$  species even at 20% vanadium loadings (Fig. 1) which might be due to the formed  $V_2O_5$  has a smaller size lies below the detection limit of XRD instrument ( $< 4\text{nm}$ ). On the other hand, the pattern of  $V/Z_{\text{CLD}}$  showed a marked overall decrease in intensity of diffraction lines due to  $V_2O_5$  agglomerates.

The lattice parameters and unit cell volume of the  $V/Z_{\text{wet}}$  and  $V/Z_{\text{CLD}}$  samples are summarized in Table 1. The data revealed an enhancement in inclusion of vanadium ions into the lattice of ZSM-5 when compared with those of vanadium ions in  $V/Z_{\text{CLD}}$ . Furthermore, increasing the lattice volume of modified samples were recognized due to the incorporation of vanadium ions which have high ionic radius ( $0.54\text{\AA}$ ) when compared with those of Si ( $0.4\text{\AA}$ ) ones. The data also show that the values of average crystallites size of ZSM-5 crystals, was calculated by Scherrer equation, and decreased following vanadium incorporation which may be due to the deposition of  $V_2O_5$  species on zeolite surfaces.

**Table 1:- The XRD characterization data of ZSM-5 zeolites prepared by CLD and wet exchange methods, as a function of increasing vanadium loadings.**

Sample	D (Å)	Unit cell				Crystallinity %
		a	b	c	V(Å) <sup>3</sup>	
ZSM-5	286.39	19.9224	20.0740	13.2288	5290.491	100
IV/ $Z_{\text{CLD}}$	360.20	19.668	20.300	13.1527	5251.352	66
IIV/ $Z_{\text{CLD}}$	322.33	19.8442	20.0428	13.302	5290.648	51
IV/ $Z_{\text{wet}}$	322.25	19.9112	20.0947	13.3934	5358.827	65
IIV/ $Z_{\text{wet}}$	313.20	19.6882	20.1480	13.3608	5299.939	64

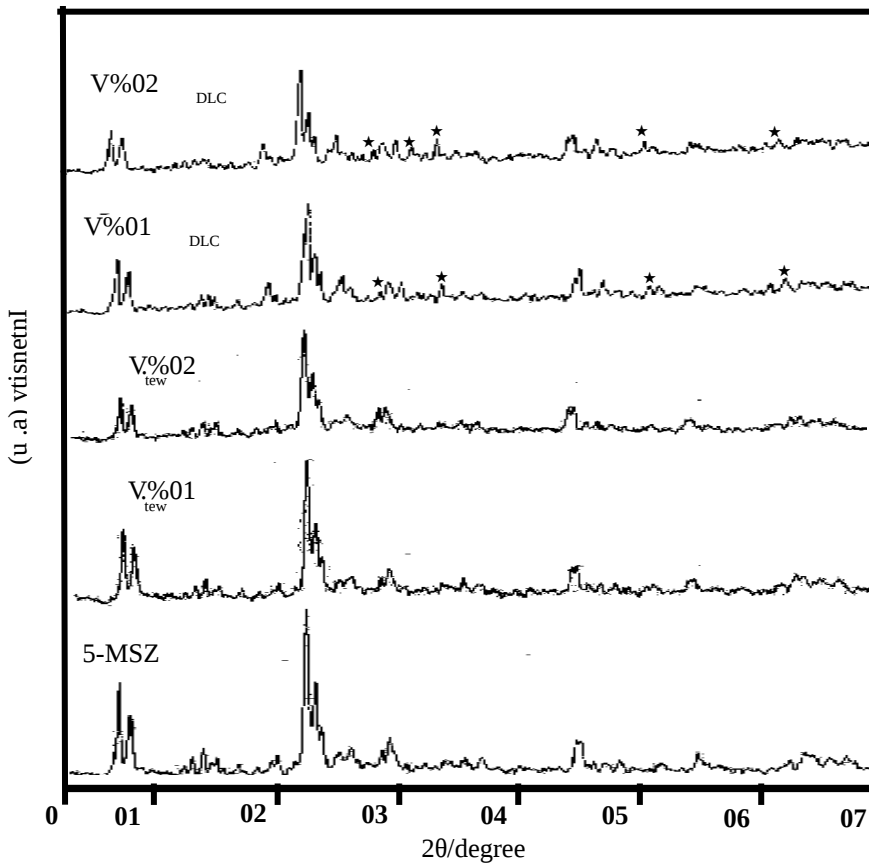


Figure (1): X-ray diffraction patterns of increasing weight percentages of  $V_2O_5$  on ZSM-5zeolite prepared by CLD and wet exchanged methods.

### Surface texture

Nitrogen adsorption - desorption data are illustrated in Table 2. The results reveal that, the decrease in  $S_{BET}$  was higher for  $V/Z_{CLD}$  samples than  $V/Z_{wet}$  ones. Similar results were also obtained for total pore volume values. This may be taken as an evidence for the location of some vanadium species deep inside pore volume of  $V/Z_{CLD}$  samples probably in an oxide form causing partial blocking. However, the devoted slight increase in pore radius of  $V/Z_{CLD}$  and  $V/Z_{wet}$  samples when compared with the parent one (21.6Å) could be indicative for penetrating V ions in the host structure of ZSM-5.

The crystal ionic radius of vanadium ion, mainly for IV coordination, is decisive to permit the ion to be localized in framework positions. The crystal ionic radius of Si (0.4Å) is apparently lower than that of V (0.54Å) and similar to that of Al (0.54Å) giving raise about the possibility of substituting V ions positions of Si<sup>4+</sup> ones rather than Al<sup>3+</sup> ions.

**Table (2): Some surface characteristics of different investigated ZSM-5 and V/Z samples, preheated at 300 °C under a reduced pressure of 10<sup>-5</sup> torr.**

Sample	S <sub>BET</sub> (m <sup>2</sup> /g)	V <sub>p</sub> <sup>total</sup> (cm <sup>3</sup> /g)	S <sup>ext</sup> (m <sup>2</sup> /g)	r <sup>-</sup> (Å)
ZSM-5	710	0.618	59.70	21.61
IV/Z <sub>CLD</sub>	560	0.484	82.48	21.80
IIV/Z <sub>CLD</sub>	549	0.499	88.07	22.90
IV/Z <sub>wet.</sub>	639	0.555	63.42	22.08
IIV/Z <sub>wet.</sub>	599	0.502	42.53	21.03

### IR spectra of samples

The FTIR spectra of ZSM-5, V/Z<sub>wet</sub> and V/Z<sub>CLD</sub> samples are shown in Fig. 2. This Figure reveals that, bands at the standard region at 1000-1300 cm<sup>-1</sup> characteristics of T-O tetrahedral and a typical pentasil zeolites for all samples and thus showing well defined bands at 798, 625, 556 and doublet at 552 of five-membered rings and 453cm<sup>-1</sup>. The IR spectrum exhibited significant bands at around 960–970 cm<sup>-1</sup>, indicating successful incorporation of the vanadium ions into the zeolite framework [20].

The IR band at 969 cm<sup>-1</sup> attributed to Si–O<sup>-</sup> linkages is related to the presence of nonextractable V<sup>5+</sup> species according to [21]. A band at 540 cm<sup>-1</sup> is shown in the IIV/Z<sub>CLD</sub> sample probably ascribed to V<sub>2</sub>O<sub>5</sub> crystallites similar to that seen when dispersing VO<sub>x</sub> on SiO<sub>2</sub> and Al<sub>2</sub>O<sub>3</sub> [22]. The intensities of bands at 556 and 552 cm<sup>-1</sup> was slightly affected and showed a decrease in intensity for IIV/Z<sub>CLD</sub> sample, broadness for IV/Z<sub>CLD</sub> sample and prominent presence of one of the doublet (552-544 cm<sup>-1</sup>) and vanishing that of the other (556 cm<sup>-1</sup>). This may give a hint about the heterogeneity of surface in these samples and rather notifying a decrease in crystallinity of these samples when compared with V/Z<sub>wet</sub> ones.

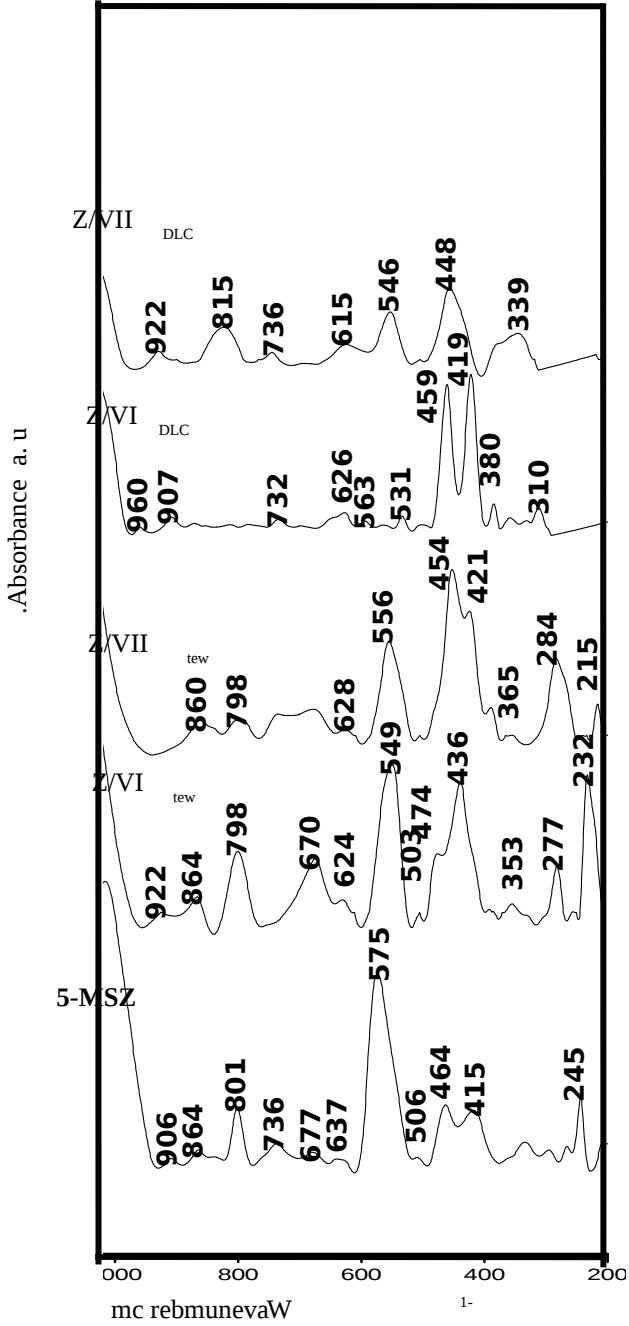


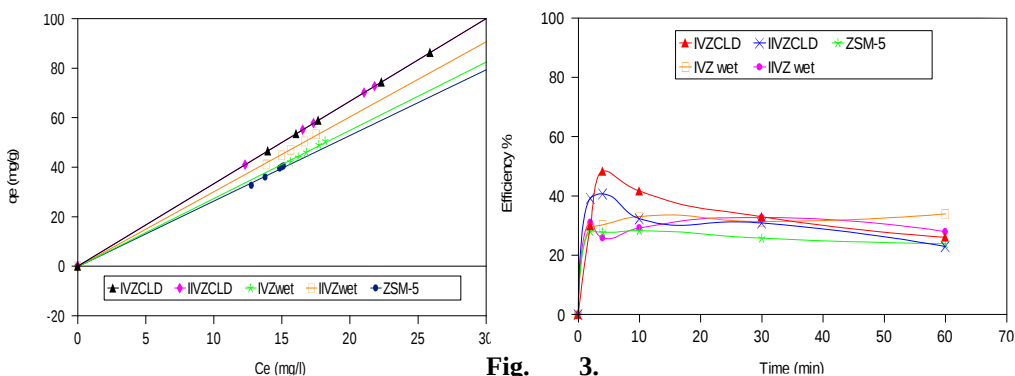


Figure (2): FTIR absorbance spectra of vanadium oxide on ZSM-5 zeolite by CLD and wet methods.

**Catalytic activity of vanadium loaded ZSM-5**

**Adsorption of DVO-4 by modified zeolite**

The influence of the adsorption processes was determined as shown in Fig. 3a; the adsorptive balance of dye of all samples could be achieved in the first 5 min of the process. Based on this result, after reaching equilibrium, about 28%, 48%, 40%, 29 and 25% of DVO-4 were adsorbed on ZSM-5, IV/Z<sub>CLD</sub>, IIV/Z<sub>CLD</sub>, I V/Z<sub>wet</sub> and II V/Z<sub>wet</sub>, respectively.



**Fig. 3. DVO-4 adsorption by ZSM-5, IV/Z<sub>CLD</sub>, IIV/Z<sub>CLD</sub>, IV/Z<sub>wet</sub> and IIV/Z<sub>wet</sub> samples. Experimental conditions: DVO 50mgL<sup>-1</sup>, catalyst 0.3 g L<sup>-1</sup>, at room temperature**

The data obtained for DVO4 adsorption using ZSM-5 and vanadium modified have been illustrated in Fig. 3b. It's clear that the samples obtained via CLD method (IV/Z<sub>CLD</sub>, IIV/Z<sub>CLD</sub>) exhibit the highest adsorption capacity (q<sub>e</sub> = 48.5 and 40.7 for IV/Z<sub>CLD</sub>, IIV/Z<sub>CLD</sub> samples respectively.) which may be due to the high amount of vanadium oxide dispersed on zeolite surface as indicated by XRD patterns (Fig.1). Furthermore, the using of V/Z<sub>wet</sub> show smallest enhancement in adsorption capacity (q<sub>e</sub> = 33 and 29 for IV/Z<sub>wet</sub>, IIV/Z<sub>wet</sub> respectively.) when compared with the parent ZSM-5 (q<sub>e</sub> = 28.5).

**Photolysis of DVO4 dye**

Aqueous solution of DVO4 dye (50 ppm) was subjected to UV irradiation, the data obtained indicate the relative stability of DVO4 dye toward UV in absence of H<sub>2</sub>O<sub>2</sub> and /or catalyst (not shown) while upon addition of H<sub>2</sub>O<sub>2</sub> as oxygen carrier material a marked increase in the degradation rate has been observed (Fig. 4).

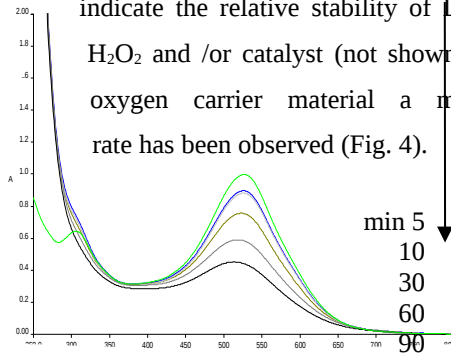


**Fig.4. UV–Vis spectral changes of the 50mgL<sup>-1</sup> DVO4 solution in photolysis process as a function of time in the presence of H<sub>2</sub>O<sub>2</sub>.**

**Degradation of DVO4 using vanadium modified ZSM-5**

The degradation of DVO4 dye by V/Z<sub>CLD</sub> and V/Z<sub>wet</sub> in presence of H<sub>2</sub>O<sub>2</sub> shown in Fig. 5. It's clear that a similar behavior result can be observed via V/Z<sub>CLD</sub> catalyst samples which exhibit the highest degradation efficiency within half min of reaction (58%, 57% respectively) this result may be attributed to high adsorption capacity of CLD samples, while V/Z<sub>wet</sub> samples exhibit 31 and 33% degradation efficiency within the same time for 10 and 20% V/Z<sub>wet</sub> respectively. The sorption rate at the initial stage was higher with V/Z<sub>CLD</sub> catalysts than those with V/Z<sub>wet</sub> due to the number of vacant sites available at the initial time on surface catalysts.

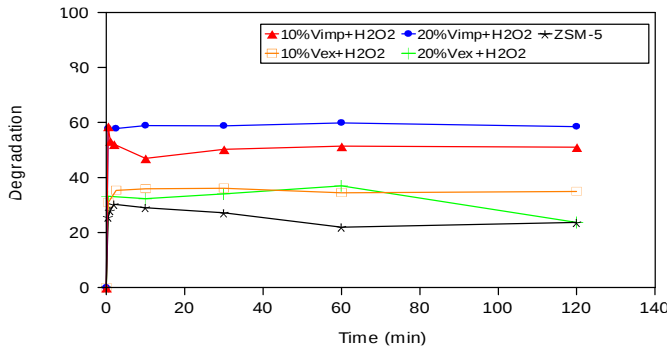
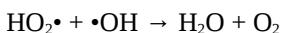
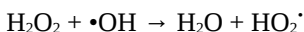


**Fig. 5. DVO-4 degradation by oxidation on ZSM-5, IV/Z<sub>CLD</sub>, IIV/Z<sub>CLD</sub>, IV/Z<sub>wet</sub> and IIV/Z<sub>wet</sub> samples.**  
**Experimental conditions: 50mgL<sup>-1</sup> dye, 0.3 g L<sup>-1</sup> catalyst, 61.6mmol/lH<sub>2</sub>O<sub>2</sub>, at room temperature**

Increasing the mineralization efficiency of dye on samples at moderate concentration (60 mmol/l) is accounted for oxidative degradation of the dye in presence of hydrogen peroxide due to H<sub>2</sub>O<sub>2</sub> may be become a scavenger of valence band holes and •OH, when present at high concentration, [23,24–27]: according to the following scheme.



As both hνB<sup>+</sup> and •OH are strong oxidants for dye, the photocatalytic oxidation will be inhibited when H<sub>2</sub>O<sub>2</sub> level gets too high. Furthermore, H<sub>2</sub>O<sub>2</sub> can be adsorbed onto zeolite particles to modify their surfaces and subsequently decrease its catalytic activity.

**photocatalytic degradation of DVO4 using vanadium modified ZSM-5**

The photocatalytic activity of DVO4 dye with IVZ<sub>CLD</sub>, catalyst appeared to be similar with IIVZ<sub>CLD</sub> as illustrated in Figs. 6, 7 (a,b) respectively.

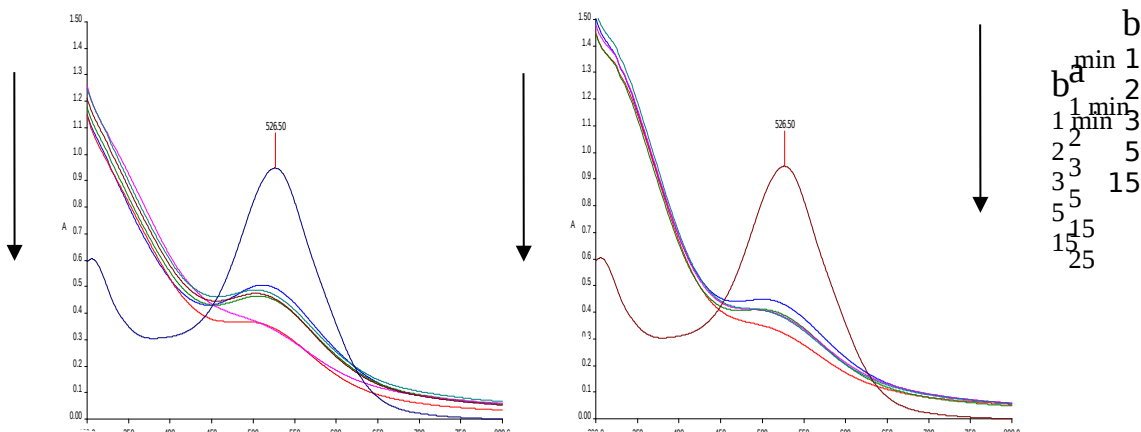


**Fig. 6a,b : UV-vis spectral changes of the 50mgL<sup>-1</sup> DVO4 solution in photodegradation process as a function of time in the presence of H<sub>2</sub>O<sub>2</sub> and (a) IVZ<sub>CLD</sub>, and (b) IIVZ<sub>CLD</sub> catalyst.**

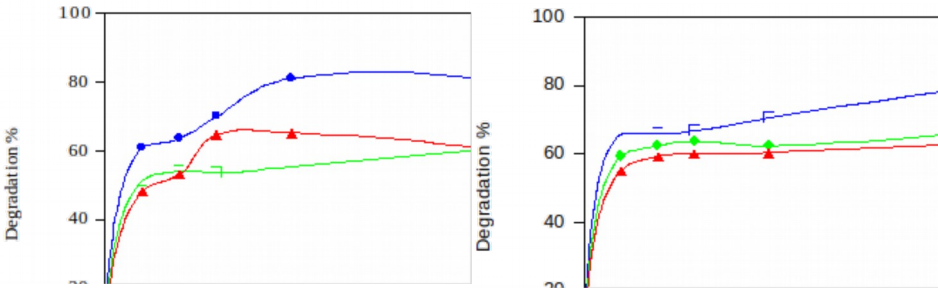


**Fig. (7) a,b : Concentration of DVO-4 changes with time as a function of varying catalyst amounts of 10, 20% V/Z<sub>CLD</sub> in presence of H<sub>2</sub>O<sub>2</sub> and UV irradiation. Kinetic and mechanism studies**

In order to compare the catalyst performances, we can be study the effect of catalyst amount then, the degradation curves can be fitted according to the Langmuir–Hinshelwood model. The initial degradation rate typically follows a pseudo-first order kinetic and the apparent rate constant can be obtained by plotting the following equation

$$\ln(C_t/C_0) = kt$$

Where  $C_0$  and  $C_t$  refer the initial and final concentration of dye at any time  $t$ , and  $k$  is the rate of pseudo-first order constant. The degradation constants could be obtained from two modified zeolite samples are resumed in Fig. 8a,b.

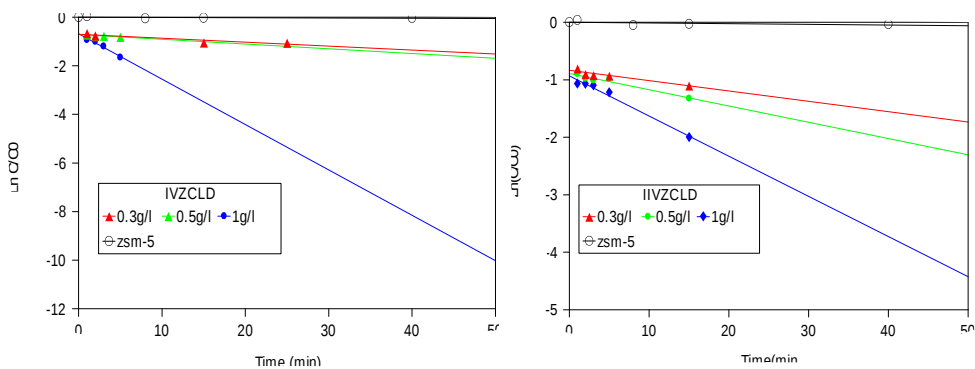


**Fig. (8) a, b: Observed pseudo first-order kinetic plots for variation loadings of V<sub>CLD</sub> on ZSM-5 for the degradation of DVO4 at the specified condition**

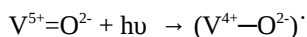
The slope of the plots produced the pseudo-first order rate constant (Table 3) show the kinetics of disappearance of DVO4 dye for an initial concentration of 50ppm under certain conditions.

**Table (3): Variation of kinetics as a function of varying Loadings on ZSM-5 as prepared by CLD method.**

Sample	Catalyst dose g/l	K(min <sup>-1</sup> )
IV/Z <sub>CLD</sub>	0.3	0.1164
	0.5	0.1255
	1.0	0.2890
IIV/Z <sub>CLD</sub>	0.3	0.1479
	0.5	0.1540
	1.0	0.1895

This Table shows that, the higher value of k when employing V/Z<sub>CLD</sub> implies the increase of active sites on these particular sample comparatively as well as enough OH radicals capable of diffusing properly to cause higher degradation rate at such low concentration.

In V/Z<sub>CLD</sub> sample vanadium atoms are in their highest oxidation state and therefore oxidatively resistant; they tend to transfer from



by UV irradiation through charge transfer from O<sup>2-</sup> to V<sup>5+</sup> of V—O—V or V=O forming excited state of charge transfer that has strong oxidation ability, and also responsible for the oxidation of azo dyes [28].

Accordingly, we believe that the degradation of the dye under UV irradiation follows two main mechanisms, which happen on the dye and on V/Z<sub>CLD</sub> catalyst respectively. Once, V/Z<sub>CLD</sub> particles are irradiated with UV light, 'OH radicals and totally oxidative degradation and mineralization of the dye substrate. The charge transfer excited state of [V<sup>5+</sup>—O<sup>-</sup>—V<sup>4+</sup>]<sup>·</sup> was a pair of a hole (O<sup>-</sup>) and a trapped electron center (V<sup>4+</sup>). O<sup>-</sup> has strong oxidation ability, and is also responsible for the oxidation of substrates.

Figure 9 shows the rate constant values; of degradation of DVO4 indicates of a pseudo-first-order kinetic model, with catalyst dose. As-first order reaction model

can describe the removal of DVO4 onto  $VZ_{CLD}$  samples, The observed increase in the removal rate when using high concentrations of  $VZ_{CLD}$  catalysts up to 0.5g/l especially those of  $IIVZ_{CLD}$  could be due to the extended specific surface areas of these samples and thus increasing the active sites

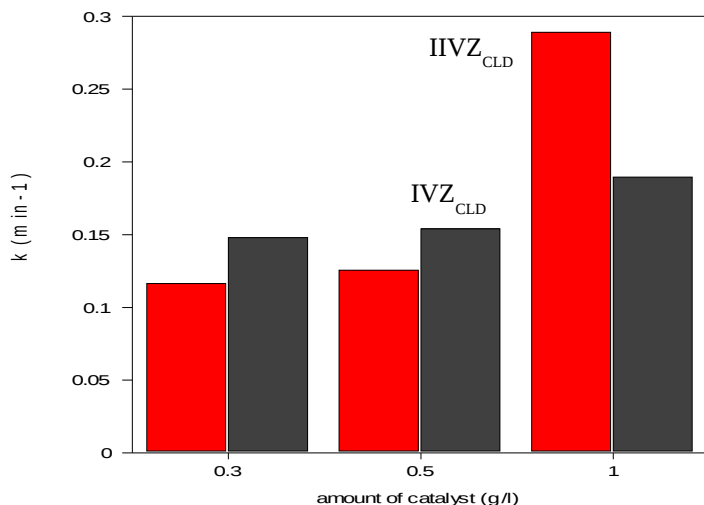


Fig. 9: K values vs. catalyst dose of  $VZ_{CLD}$  samples.

## Conclusion

The analysis of FT-IR, XRD pattern and photolysis results obtained for V-containing MFI zeolites clearly illustrates the key role of vacant T-sites and mononuclear V ions in the incorporation of vanadium into zeolite materials. From results reported recently, it can be concluded that V-containing microporous materials are active in photooxidation and their activity can be related to the presence of isolated vanadium species. Results showed that the addition of  $V/Z_{CLD}$ ,  $V/Z_{wet}$  and  $H_2O_2$  to the dye solution enhanced the rate of degradation. The decolorization followed the pseudo first order kinetics model and a significant mineralization of (DVO-4) was observed.

**References**

1. H. Park and W. Choi, *J. Photochem. Photobiol. A: Chem.*, 159 (2003) 241–247.
2. N. Daneshvar, D. Salari and A.R. Khataee, *J. Photochem. Photobiol. A: Chem.*, 157 (2003) 111–116.
3. D.F. Ollis, E. Pelizzetti and N. Serpone, *Environ. Sci. Technol.*, 25 (1991) 1523.
4. Y. Anjaneyulu, N. Sreedhara Chary and D. Samuel Suman Raj, Decolourization of industrial effluents–available methods and emerging technologies–a review, *Rev. Environ. Sci. Biotechnol.*, 4 (2005) 245–273.
5. J.G. Yu, J.C. Yu, W.R. Ho and Z.T. Jiang, *J. Chem.*, 26 (2002) 607.
6. J.C. Crittenden, Y. Zhang, D.W. Hand, D.L. Perram and E.G. Marchand, *Water Environ. Res.*, 68 (1996) 270.
7. Huang Y, Li J, Ma W, Cheng M, Zhao J. Efficient H<sub>2</sub>O<sub>2</sub> oxidation of organic pollutants catalyzed by supported iron sulfophenylporphyrin under visible light irradiation. *J Phys Chem B*, 108 (2004) 7263–7270.
8. A. Corma, *Chem. Rev.*, 97 (1997) 2373, and references therein.
9. A.C. Akah, G. Nkeng and A.A. Garforth, The role of Al and strong acidity in the selective catalytic oxidation of NH<sub>3</sub> over Fe-ZSM-5, *Appl. Catal. B*, 74 (2007) 34–39.
10. J.Y. Wang, F.Y. Zhao, R.J. Liu and Yong-Qi Hu, Oxidation of cyclohexane catalyzed by metal- containing ZSM-5 in ionic liquid, *J. Mol. Catal. A*, 279 (2008) 153–158.
11. P.O. Graf and L. Lefferts, Reactive separation of ethylene from the effluent gas of methane oxidative coupling via alkylation of benzene to ethylbenzene on ZSM-5, *Chem. Eng. Sci.*, 64 (2009) 2773–2780.
12. A. Miyamoto, D. Medhanayn and T. Inui, *Appl. Catal.*, 28 (1986) 89.
13. T. Inui, D. Medhanavyn, P. Praserthdam, K. Fukuda, T. Ukawa, A. Sakamoto and A. Miyamoto, *Appl. Catal.*, 18 (1985) 311.
14. S. Bordiga, S. Coluccia, C. Lamberti, L. Marchese, A. Zecchina, F. Boscherini, F. Buffa, F. Genoni, G. Leofaniti, G. Petrini and G. Vlaic, *J. Phys. Chem.*, 98 (1994) 4125.
15. F. Cavani, F. Trifiro, P. Jiru, K. Habersberger and Z. Tvaruzkova, *Zeolites*, 8 (1998) 12.
16. M. Iwamoto, H. Yahiro, N. Mizuno, W. X. Zhang, Y. Mine, H. Furu Kawa and S. Kagawa, *J. Phys. Chem.*, 96(1992)9360.
17. P. Klug and L.E. Alexander, *Direction Procedures for Polycrystalline and Amorphous Materials*, Wiley, New York, (1954).
18. A.M. Daifullah and M.M. Mohamed, *J. Chem. Technol. Biotechnol.*, 79 (2004) 468.
19. M.R. Ghezzar, F. Abdelmalek, M. Belhadj, N. Benderdouche and A. Addou, *Appl. Catal. B.*, 71 (2007) 304.

20. G. Centi, S. Perathoner, F. Trifiró, A. Aboukais, C.F. Aiss and M. Gueltin, *J. Phys. Chem.*, 96 (1992) 2617.
21. T. Sen, P. R. Rajamohanan, S. Ganapathy, and S. Sivasanker., *J. of Catalysis.* 163,(1996) 354–364.
22. B. Olthof, A. Khodakov, A. T. Beu and E. Iglesia, *J. Phys. Chem. B* : 104 (2000)1516.
23. N. Daneshvar, D. Salari and A.R. Khataee, *J. Photochem. Photobiol.A: Chem.*, 157 (2003) 111.
24. O. Legrini, E. Oliveros and A.M. Braun, *Chem. Rev.*, 93 (1993) 671.
25. M.W. Peterson, J.A. Tuner and A.J. Nozik, *J. Phys. Chem.*, 95 (1991) 221.
26. S. Malato, J. Blanco, C. Richter, B. Braun and M.I. Maldonado, *Appl. Catal. B: Environ.*17 (1998) 347.
27. D.I. Petkowicz , Sibebe B.C., Carlos D. Silva, Zênis N. da Rochac and João H.Z. dos Santosa *Chemical Engineering Journal.*, 158 (2010) 505–512.
28. Y. Yang, Y. Guo, C. Hu, Y. Wang and E. Wang, *Appl. Catal. A*, 273 (2004) 201.